International Atomic Energy Agency

INDC(CCP)-315/L

INDC INTERNATIONAL NUCLEAR DATA COMMITTEE

DIFFERENTIAL NEUTRON EMISSION AND INELASTIC CROSS SECTION FROM ^{208}Pb AND ^{209}Bi AT 14.1 MeV INCIDENT ENERGY

S.P. Simakov, B.V. Devkin, M.G. Kobozev, V.P. Lunev,
A.A. Lychagin, V.A. Talalaev, N.N. Titarenko, A.B. Zeleneckij,
B.V. Zhuravlev
Institute of Physics and Power Engineering, Obninsk, USSR

T. Starichkai
Institute of Experimental Physics, Debrecen, Hungary

September 1990

IAEA NUCLEAR DATA SECTION, WAGRAMERSTRASSE 5, A-1400 VIENNA

INDC(CCP)-315/L

DIFFERENTIAL NEUTRON EMISSION AND INELASTIC CROSS SECTION FROM ^{208}Pb AND ^{209}Bi AT 14.1 MeV INCIDENT ENERGY

S.P. Simakov, B.V. Devkin, M.G. Kobozev, V.P. Lunev,
A.A. Lychagin, V.A. Talalaev, N.N. Titarenko, A.B. Zeleneckij,
B.V. Zhuravlev
Institute of Physics and Power Engineering, Obninsk, USSR

T. Starichkai
Institute of Experimental Physics, Debrecen, Hungary

September 1990

Reproduced by the IAEA in Austria
September 1990

90-04595

DIFFERENTIAL NEUTRON EMISSION AND INELASTIC CROSS SECTION FROM ^{208}Pb AND ^{209}Bi AT 14.1 MeV INCIDENT ENERGY.

S.P. Simakov, B.V. Devkin, M.G. Kobozev, V.P. Lunev, A.A. Lychagin, V.A. Talalaev, N.N. Titarenko, A.B. Zeleneckij, B.V. Zhuravlev

Institute of Physics and Power Engineering, Obninsk, USSR

T. Starichkai

Institute of Experimental Physics, Debrecen, Hungary

Abstract.

The double differential cross-section of $^{208}Pb(n,n_{emission})$, $^{209}Bi(n,n_{emission})$ and $^{208}Pb(n,n'\gamma)$ reactions at 14.1 MeV incident neutron energy have been measured by time of flight method. The experimental arrangement, measuring and data reduction procedures are described. The cross-section obtained are compared each others and with theoretical calculations basing on compound and direct reaction models.

1. Introduction.

The Double Differential neutron emission cross-section (DDCS) at 14 MeV incident energy from lead and bismuth are rather important with applied and basic points of views. The particular feature of these nuclei is that the (n,2n) reaction has a dominant contribution (90% [1]) in total nonelastic cross-section. Therefore lead is supposed to be used as a neutron multiplier in conceptual designs of fusion reactors. According to this applied purposes the DDCS at 14 MeV have to be known with about 20% accuracy [2].

The theoretical interest to these two adjacent nuclei is caused by the following aspects. ^{208}Pb is a double-closed-shell nucleus, on the other hand the neighboring element ^{209}Bi has a valence protons in $h_{9/2}$ shell. It is known that some low lying levels in ^{209}Bi can be described in the model of weak coupling of valence proton with the vibration states in magic core ^{208}Pb, but others levels - as single particle/hole transitions [3]. The comparison of neutron experimental spectra from ^{208}Pb and ^{209}Bi

can give the information about what kind of states populated in neutron non-elastic reactions, the validity of weak coupling model and difference of level density function.

Besides the (n,2n) reaction, (n,n'γ) reaction contributes practically another part (10%) of non-elastic cross-section for these nuclei. The competition between the (n,2n) and (n,n'γ) channels depends on gamma and neutron decay widths at excitation energy of target nucleus just above the neutron binding energy. So we decided to measure the spectra of neutrons from the ^{208}Pb(n,n'γ) reaction to make conclusion about these values.

In this paper we summarize the results of a few our previous experiments (except neutron emission cross-section from ^{208}Pb), so the details can be find elsewhere [4-6].

2. Experiment.

The differential neutron emission and inelastic cross-sections have been measured by time of flight (TOF) method on fast neutron spectrometer based on pulsed neutron generator KG-0.3 IPPE [5]. During the experiments energy of accelerated deutrons was 250 keV, ion pulses width of 2.5 ns with repetition period 400-800 ns and mean deutron beam about 1 μA. The neutron yield of about 10 sec was produced in an air cooled solid TiT target.

In the case of DDCS measurements the experimental set-up is shown in fig. 1. The measurements have been performed with short (2-4 m) and long (7 m) flight paths. The advantage of short path is a larger spectrometer aperture and independence of initial neutron energy versus the scattering angle, but at long path we have better energy resolution. Taking this into account we measured low energy part (0.5 - 10 MeV) of the spectra at short flight path and high energy (3 - 14 MeV) - at long. Some parameters of particular experiments are listed in table 1.

Scattered neutrons were registered by a detector consisted of a NE-218 liquid scintillator (Ø10 × 5 cm) coupled with XP-2041 photo multiplier. During the measurements at short flight path, detector was housed in a massive shield composed of paraffin and LiH mixture. The direct neutron flux from the target was attenuated by a shadow bar of iron and copper. The shield could be automatically rotated around the sample to perform the

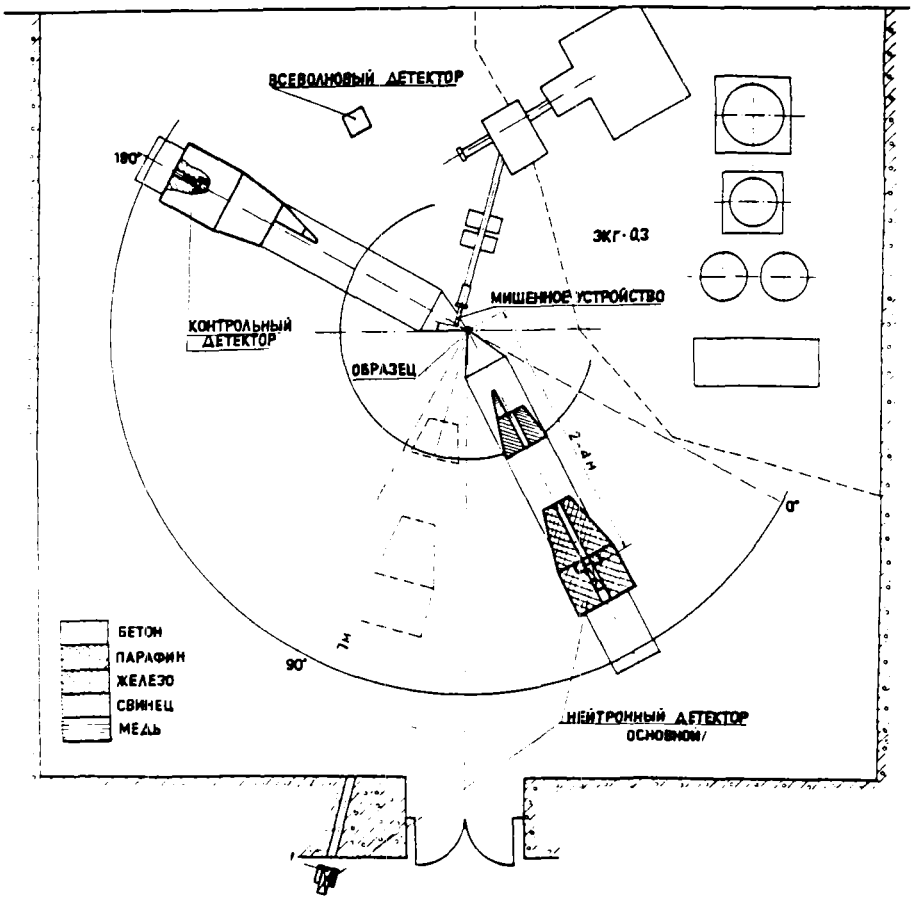

Fig. 1. Lay-out of expreriment for measuring the neutron emission specta at short (2 - 4 m) and long (7 m) flight path.

Table 1. Parameters of experiments.

Nucleus	^{208}Pb			^{209}Bi	
Reaction	Emission		(n,n'γ)	Emission	
Incident energy, MeV	14.1	13.4-14.8	14.1	14.1	13.4-14.8
Resolution,MeV (at 14 MeV)	1.2	0.6	2	2	0.6
Flight path,m	3.1	7.1	2.2	2.2	7.1
Detector bias, MeV	0.2	1.6	0.2	0.2	1.6
Angles, degrees Step	30-150 30	30 - 150 15	60-120	30-150 30	30-150 30
Sample size,cm	Ø4.5×Ø3×5		Ø7.6×Ø5×1	Ø5×Ø4×5	

measurements at different angles. In the case of long path, the detector was installed in lead house behind the concrete wall. The angle of scattering was changed by shifting the sample along the collimator axis, resulting in 10% changing of incident neutron energy.

Principle of experimental selection of neutrons from $^{208}Pb(n,n'\gamma)$ reaction consists of registration of neutrons in coincidence with the gamma quanta of specific energy. In the case of ^{208}Pb it is known, that with probability of 95-99% [8] its excited states feed by gamma cascade the lower 2.61 MeV 3^- state. Thus the spectra of neutrons measured in coincidence with 2.61 MeV gammas will correspond the $^{208}Pb(n,n'\gamma)$ reaction.

The lay-out of this type experiment is shown in fig. 2. For the detection of gammas we used NaJ (Ø10 × 10 cm) plus FEU-141 photo multiplier scintillator detector. The ring sample had a such size that to receive the maximum count rate (about 10 true events/hour) and to shield both neutron and gamma detectors from target direct flux by shadow bars.

The detectors' outputs were fed into CAMAC electronic modules connected on line with SM-1420 computer. Anode pulses were used for fast constant fraction timing (start) as well as for gamma-neutron pulse shape discrimination. Stop pulses were obtained from the pick-up electrode located before the target.

In the case of $^{208}Pb(n,n'\gamma)$ measurements, the electronic block-scheme, at first, select gammas from neutrons by time of flight. Then selected events fed amplitude analyzer. Two windows were set up in energy gamma spectrum. The first corresponds the 2.61 MeV energy, the second - a little higher. The time of flight of neutrons coincident with these two windows was recorded in different memory groups as effect+background and background.

The neutron generator pulse mode was controlled by time of flight monitor consisted of fast plastic scintillator СПС-I5Б (Ø 2 × 2 cm) and FEU-87. The time resolution of this detector was 0.4 ns. For monitoring neutron yield from the target and making possible normalization of different runs a Long Counter was used.

The neutron detector efficiency was experimentally determined by three methods. In the first one, a specially designed ^{252}Cf ionization chamber (about 10^5 fission rate) replaced the sample. Spectrum of prompt fission neutrons was measured by TOF method. The detector efficiency was then reduced from comparison of measured spectrum with standard one [10].

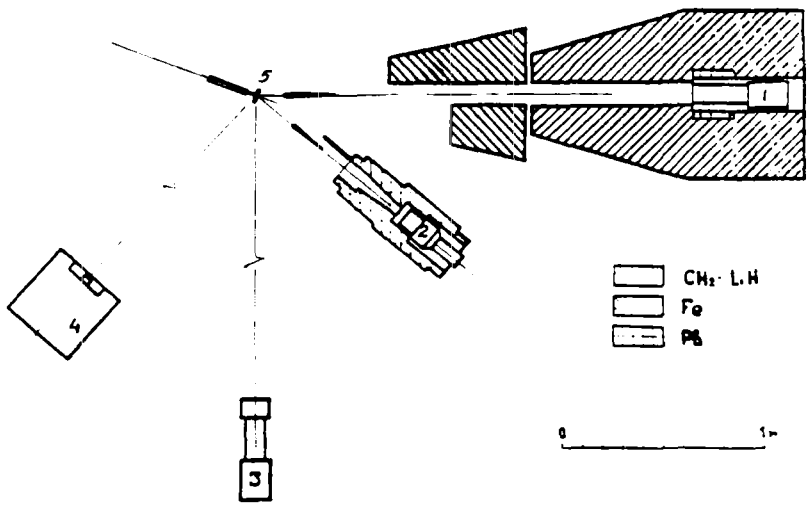

Fig. 2. Lay-out of experiment for measuring the neutron spectra from (n,n'γ) reaction. 1 - neutron detector, 2 - gamma detector, 3 - TOF monitor, 4 - Long Counter, 5 - sample.

In the neutron energy region above 6 MeV, where the statistical accuracy with ^{252}Cf source becomes poor, the efficiency was measured relative to n-p scattering cross-section [10]. In this case we placed at the same spot a fast scintillator (stilben $\varnothing$ 1 × 4 cm) detector, that gave the stop pulses for the TOF separation of hydrogen scattered neutrons.

At 14 MeV neutron energy the efficiency was measured by associated alpha particle method. The spectrum of alphas was registered by silicon surface barrier detector.

Conversion from the neutron spectra to DDCS was accomplished by comparison with the n-p scattering cross-section (as described above) and by aluminum foil activation method. In the later case Al foils replaced the sample and were irradiated , the target neutron yield been monitoring by Long Counter. The activity of irradiated foils was then measured by $\beta-\gamma$ coincidences spectrometer. These data and the standard $^{27}Al(n,\alpha)$ reaction cross-section [10] were used for calculation of the incident neutron flux at the sample position.

3. Experimental results.

The angle-integrated DDCS are listed in table 2 in centrum mass system. It was mentioned above that emission cross-sections have been measured at two different flight paths and thresholds. In neutron energy range less then 4 Mev we took the short path

data, above 6 MeV - long and in medium region - the mean. Moreover, the long path data , measured at different incident energy, were transformed to one energy 14.1 MeV. The inelastic scattering cross-section of $^{208}Pb(n.n'\gamma)$ reaction, listed in table 2, is experimentally integrated over angle range 60^{o}- 120^{o} as a result of experimental geometry (fig. 2).

Table 2. Angle-integrated cross-sections and absolute errors in centrum mass system.

NN	E,MeV	$^{209}Bi(n,n_{emiss})$	$^{208}Pb(n,n_{emiss})$	$^{208}Pb(n,n'\gamma)$
1	0.6	1873 ± 133	1963 ± 121	
2	0.8	1927 ± 135	1913 ± 117	
3	1.0	1884 ± 132	1810 ± 110	
4	1.2	1810 ± 126	1710 ± 104	
5	1.4	1720 ± 121	1564 ± 95	
6	1.6	1608 ± 113	1415 ± 86	
7	1.8	1474 ± 104	1267 ± 77	
8	2.0	1329 ± 94	1121 ± 68	
9	2.2	1184 ± 84	993 ± 61	
10	2.4	1047 ± 75	832 ± 51	
11	2.6	917 ± 66	664 ± 41	
12	2.8	782 ± 56	548 ± 35	
13	3.0	659 ± 48	457 ± 29	
14	3.2	554 ± 41	376 ± 25	
15	3.4	470 ± 34	325 ± 22	
16	3.6	396 ± 29	305 ± 20	
17	3.8	329 ± 24	285 ± 18	
18	4.0	274 ± 17	250 ± 16	
19	4.2	240 ± 15	219 ± 14	
20	4.4	203 ± 13	195 ± 12	
21	4.6	178 ± 11	170 ± 11	8 ± .4
22	4.8	158 ± 10	148 ± 10	24 ± 10
23	5.0	133 ± 9	131 ± 9	33 ± 12
24	5.2	118 ± 8	113 ± 8	36 ± 12
25	5.4	100 ± 7	97 ± 7	41 ± 12
26	5.6	84 ± 6	89 ± 6	43 ± 11
27	5.8	81 ± 6	83 ± 6	40 ± 11
28	6.0	80 ± 6	78 ± 6	43 ± 11
29	6.2	71 ± 5	75 ± 6	49 ± 11
30	6.4	67 ± 5	71 ± 6	50 ± 11
31	6.6	56 ± 4	67 ± 5	50 ± 11
32	6.8	56 ± 4	64 ± 5	51 ± 11
33	7.0	56 ± 4	62 ± 5	56 ± 11
34	7.2	66 ± 5	61 ± 5	60 ± 11
35	7.4	66 ± 5	60 ± 5	62 ± 11

Table 2. (continued)

NN	E,MeV	$^{209}Bi(n,n_{emiss})$	$^{208}Pb(n,n_{emiss})$	$^{208}Pb(n,n'\gamma)$
36	7.6	68 ± 5	61 ± 5	64 ± 11
37	7.8	65 ± 5	62 ± 5	67 ± 11
38	8.0	67 ± 5	64 ± 5	71 ± 11
39	8.2	65 ± 5	66 ± 5	76 ± 12
40	8.4	73 ± 6	68 ± 6	77 ± 12
41	8.6	69 ± 5	69 ± 6	76 ± 11
42	8.8	72 ± 5	66 ± 6	74 ± 11
43	9.0	68 ± 5	63 ± 5	69 ± 11
44	9.2	67 ± 6	61 ± 5	62 ± 11
45	9.4	81 ± 6	66 ± 6	61 ± 11
46	9.6	85 ± 6	71 ± 6	59 ± 10
47	9.8	67 ± 5	72 ± 6	59 ± 10
48	10.0	61 ± 5	62 ± 6	59 ± 10
49	10.2	51 ± 4	50 ± 5	60 ± 10
50	10.4	31 ± 4	39 ± 5	
51	10.6	37 ± 3	34 ± 4	
52	10.8	37 ± 4	34 ± 4	
53	11.0	39 ± 4	40 ± 4	
54	11.2	55 ± 4	49 ± 5	
55	11.4	69 ± 5	54 ± 5	
56	11.6	54 ± 5	48 ± 5	
57	11.8	30 ± 3	36 ± 6	
58	12.0	29 ± 3	24 ± 5	
59	12.2	18 ± 2	16 ± 4	
60	12.4	17 ± 2	13 ± 4	
61	12.6	17 ± 2		
62	12.8	14 ± 3		

The energy-angle-integrated cross-sections are listed in table 3. Extrapolation of cross-section below the detector threshold was made using the models calculations described below.

Table 3. Energy-angle-integrated cross-sections, Q-energy and maximum energy of neutrons from (n,2n) reaction.

Nucleus	^{208}Pb	^{209}Bi
σ_{emis}, mb	5160 ± 300	5220 ± 310
$\sigma_{nn'\gamma}$, mb	405 ± 30	
σ_{n2n}, mb	2380 ± 140	
Q_{n2n}, MeV	- 7.37	-7.45
E_{n2n}, MeV	6.64	6.55

The experimental data are corrected for neutron flux attenuation and multiple scattering in the samples. These corrections were calculated by Monte-Karlo code SSE using the evaluated or experimental neutron data [1]. The uncertainties of experimental data include statistics (3-50%), detector efficiency error (5%) and absolute normalization error (4%).

The comparison of DDCS from ^{209}Bi is made with data of Pavlik and Vonach [10], who evaluated the data of 4 experiments. The deviation of present experiment results from [11] does not exceed 10%, except the high energy part of spectrum, where data [11] have worse energy resolution. The high energy resolution experimental data of Takahashi e.a. [12] have been measured only at two angles and was not corrected for multiple scattering effects. Discrepancy between our and [12] data somewhere have a value of 50% or more.

The differential neutron emission and inelastic scattering cross-section from pure isotope ^{208}Pb have not been measured previously.

4. Theoretical calculations and analyze of experimental results.

The reaction cross-sections were calculated in the framework of compound and direct mechanisms. The statistical part of reactions were calculated using Hauser-Feshbach model, including angular momentum and parity conservation, competition between the neutrons, gammas and charge particles emission. We calculated the neutron emission coefficients with optical model potential of Rapaport e.a. [13] for lead and of Lawson e.a. [14] for bismuth. The transition to the discrete levels of residual nuclei was taken into account. For example: 20 states till the excitation energy U = 4.2 MeV for the ^{208}Pb and 40 states till U = 3.6 MeV for ^{209}Bi [8]. At the higher excitation energies level density function, taking into account shell,superfluid and collective effects [15], was used. The radiation strength functions for $E\lambda$ and $M\lambda$ transitions, determing the gamma-neutron competition, were calculated in Axel-Brink model. Its absolute normalization corresponds the experimental observed radiation width at neutron binding excitation energy [16].

The direct neutron inelastic scattering cross-section was estimated using a coupled-channel model and distorted wave Born approximation. Form-factors of the direct transitions were calculated in Bohr-Mottelson model for collective excitation

modes. The excitation energies, deformation parameters of vibration states in ^{208}Pb was taken from the similar analyze of $^{208}Pb(p,p')$ reaction [17]. The same parameters was taken for ^{209}Bi (the model of weak coupling $h_{9/2}$ proton with vibration states of magic core ^{208}Pb).

The experimental angular-integrated neutron emission spectra from ^{208}Pb and ^{209}Bi are shown in fig. 3. As can be seen these spectra practically coincide each other in the whole energy region (in the insert of fig. the ratio of ^{209}Bi cross-section to ^{208}Pb one is shown). The angular distributions of secondary neutrons agree for these two nuclei as well (fig. 4).

Therefore , from the comparison of DDCS we can make conclusion that adding of one proton to closed-shell ^{208}Pb does not influence on energy/angle distributions of secondary neutrons. What does it mean with physical point of view ? We can receive the answer after comparison of experimental and calculated data.

Such comparison is shown in figs. 4 and 5. It is seen that compound component describes the low-energy part of spectra. The agreement of spectra from both nucleus means the equal energy dependence of level density functions for the residual nucleus.The direct component contributes to the high energy part and satisfactory describes the excitation of the first 3^- state. Thus we can make conclusion that in direct inelastic scattering only the collective states are practically excited, and weak coupling model is a good approximation for the ^{209}Bi.

In the intermediate energy region the theoretical model calculation underestimate experimental DDCS. The difference between experimental spectra and compound one is estimated to be 350 mb, whereas the total direct cross-section equal 210 mb. The remained part (40%) of nonequilibrium process can result from the missed in calculation collective or single particle states, or from more complicated multi-step processes.

The spectrum of neutrons from reaction $^{208}Pb(n,n'\gamma)$ is shown in fig. 5. For neutron energies above E_{n2n}=6.64 MeV (maximum energy from (n,2n) reaction) the spectrum of inelastically scattered neutrons have to coincide with the emission neutron spectrum. In lower energy region (when excitation of ^{208}Pb after the emission of first neutron exceeds the neutron binding energy) the contribution of neutrons from $(n,n'\gamma)$ and (n,2n) reactions becomes energetically possible.

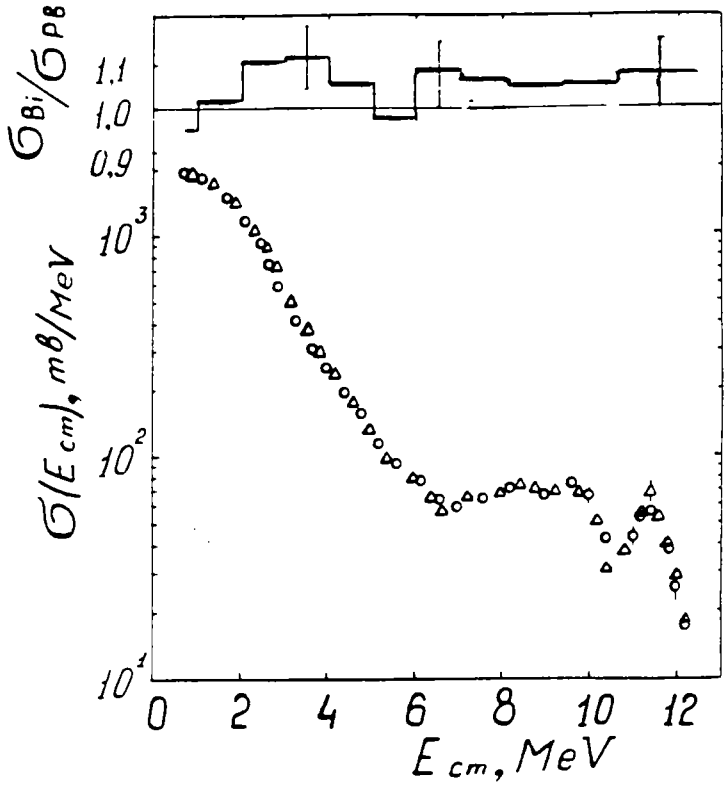

Fig. 3. Angle-integrated neutron emission spectra from 208-Pb (o) and 209-Bi (Δ). In In the insert its ratio is shown.

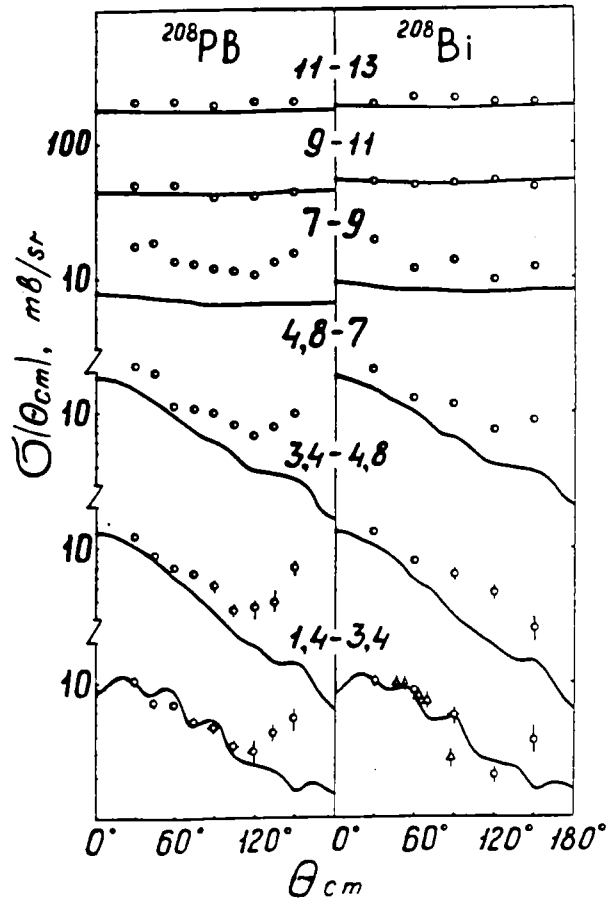

Fig. 4. Energy integrated neutron emission cross sections.
Experiment: o - present work, Δ - [18].
Calculation: —— -sum of compound and direct components.

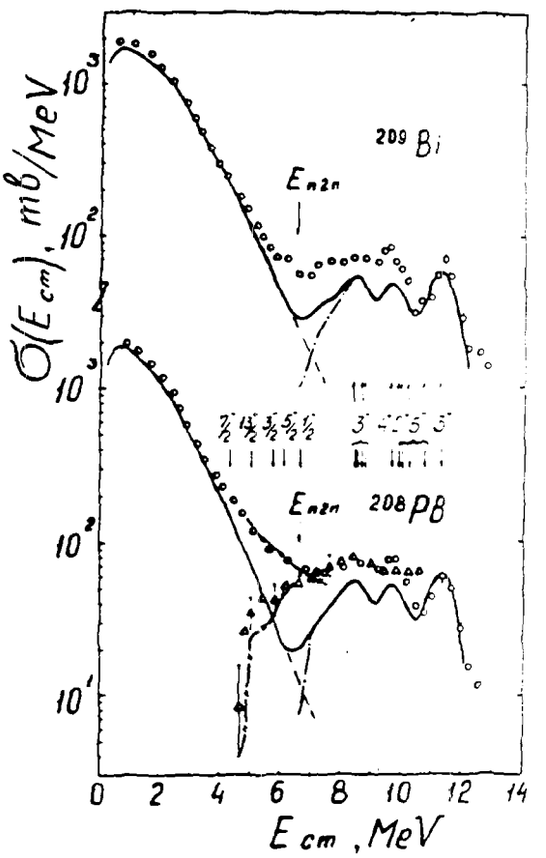

Fig. 5. Comparison of experimental and calculated data.
Experiment: o - angle-integrated neutron emission cross-sections,
Δ - inelastically scaterred neutrons.
Calculations: – – – – compound component,
–·–·– - direct component,
——— - its sum.
–//–//– - (n,n'γ) spectrum

It is interesting to notice that inelastic scattering spectrum sharply decrease with decreasing of neutron energy at 5 Mev but not at E_{n2n}. In the fig.5 it is seen that this critical point corresponds the possibility of population of high spin level $13/2^+$ (U=1.68 MeV) in reaction $^{208}Pb(n,2n)^{207}Pb$. This effect can be described if one take into account the total spin conservation law. The high orbital momentum (about 12/2), input by 14 MeV neutron, can not be compensated by two neutrons with total energy less or equal E_{n2n}. Therefore $^{208}Pb(n,2n)$ reaction will populate with higher probability the high spin states.

These qualitative explanation is confirmed by statistical model calculation, in which the gamma-neutron competition and spin conservation law are taken into account. Since the sum of compound and direct cross-section underestimates the experimental one in energy region under interest, we introduced precompound emission

of the first neutron. As can be seen in fig. 5, the spectrum of inelasticaly scattered neutrons is satisfactory described. It is interesting to notice that reaction $^{208}Pb(n,n'\gamma)$ with 20% probability results in population of unbound states in ^{208}Pb. It means that sum energy of gammas from this reaction have to be about 0.7 MeV larger in comparison with case when gamma competition is absent.

References.

1. Neutron Cross Section. Academic Press. INC, New York, 1988
2. World Request List for Nuclear Data. INDC(SEC)-88/USRF, IAEA, Vienna, 1983
3. W.T. Wagner e.a. Phys. Rev., 1975, v. C12, p. 757
4. A.A. Lychagin e.a. Proc. of. V Intern. Conf. on Neutron Induced Reactions (Smolenice, 1988), p. 272
5. S.P. Simakov e.a. Ibid, p.266.
6. Б.В.Девкин и др. Вопросы атомн.наукии техн.Се. Ядерн. константы. I989, вып. 2, с. I9.
7. В.Б. Ануфриенко и др. Там же. Сер. Реакторостроениею I977,вып. 5(I9), с. 34
8. C.M. Lederer, V. Shirtley. Tables of Isotopes. New York, 1978
9. W. Mannhart. Report IAEA-TECDOC-410, Vienna, 1987, p.158
10. Data Standards for Nuclear Measurements. Report IAEA-TECDOC-227, IAEA, Vienna, 1983
11. A. Pavlik, H. Vonach. Physics Data,1988, n° 13-14
12. A. Takahashi e.a. Report A-87-01, Osaka, 1987
13. J. Rapaport e.a. Nucl. Phys., 1979, v. A330, p. 15
14. R.D. Lawson e.a. Phys. Rev., 1987, v. C36, p. 1298
15. О.Т. Грудзевич и др. Нейтронная физика. М.,ЦНИИАИ. I988,т.2, с. 96
16. В.М. Бычков и др. Вопросы атомн. науки и техн. Сер. Ядерн. константы, I987, вып. 3, с. I4
17. W.T. Wagner e.a. Phys. Rev., 1975, v. C11, p. 486
18. P.H. Stelson e.a. Nucl. Phys., 1965. v. 68, p. 97